# Dynamic DNA Damage and Repair Modeling: Bridging the Gap between Experimental Damage Readout and Model Structure

Mathias S. Weyland[1,5], Pauline Thumser-Henner[2,3,4], Carla Rohrer Bley[2,3], Simone Ulzega[1], Alke Petri-Fink[5,6], Marco Lattuada[6], Stephan Scheidegger[1], and Rudolf M. Füchslin[1]

[1] Zurich University of Applied Sciences Winterthur, Switzerland
[2] Division of Radiation Oncology, Vetsuisse Faculty, University of Zurich, Zurich, Switzerland
[3] Center for Applied Biotechnology and Molecular Medicine (CABMM), University of Zurich, Zurich, Switzerland
[4] Center for Clinical Studies, Vetsuisse Faculty, University of Zurich
[5] BioNanomaterials Group, Adolphe Merkle Institute, University of Fribourg, Fribourg, Switzerland
[6] Department of Chemistry, University of Fribourg, Fribourg, Switzerland

**Abstract.** In this work, a method is presented to map a set of experimentally obtained, time-resolved distributions to a dynamic model. Specifically, time-resolved comet assay readouts of cancer cells after application of ionizing radiation are mapped to the Multi-Hit-Repair model, a radiobiologically motivated dynamic model used to predict DNA damage and repair. Differential evolution is used for parameter-search to showcase the potential of this method, producing a prediction close to the experimental measurement. The results obtained from the parameter search are used to characterize aspects of the repair process. The method is compared to prior attempts of finding model parameters from dose-response curves, revealing that calibration is required to render the two comparable.

**Keywords:** Dynamic DNA damage/repair model · comet assay (single cell gel electrophoresis) · differential evolution

## 1 Introduction

Radiotherapy is a cancer treatment in which tumors are targeted with high doses of ionizing radiation to eradicate the cancer cells. The treatment induces DNA damage which the cells attempt to repair in order to avoid eradication. This repair process can be characterized with the help of biologically inspired dynamic models. These models have parameters such as radiosensitivity, speed and efficiency of repair; the corresponding parameter values can be used to gain insights into the nature of the repair process and to characterize cancer- and

normal tissue cell lines. Knowing more about these aspects of cancer ultimately leads to novel or optimized treatments for cancer.

A critical property of DNA damage in cells is that it is not deterministic: When a number of cells are irradiated, the specific damage is very different in each of the cells due to the stochastic nature of the process [3]. In consequence, damage induction in cells, as well as their individual reaction to it, will vary even when they are selected from a genetically well defined cell line and irradiated homogeneously. This variation is concealed to some extent when only mean values and standard errors are reported. Sometimes, it is of importance to consider how data are distributed, and how these distributions change over time. As explained below, DNA damage and repair is such a case. More generally, distributions are reflecting some aspects of complexity in the system: A population of genetically identical or similar entities (e.g. cells) will divide into sub-populations which start to evolve differently. When modelling such complex systems, modellers are often confronted with model parameters that cannot be determined uniquely by fitting the average behaviour of experimentally observed populations.

In this broader context, the strategy presented here can be applied not only to DNA damage and repair, but rather to any situation where data distributions in a time-resolved context are paramount. The example of DNA damage and repair chosen here to showcase the method is a good example for the following reason: If little damage is introduced to a cancer cell, the probability of a successful repair is high. After repair, this cell is able to undergo mitosis, contributing to the progression of cancer. Even if only a small number of cancer cells reach this state, the consequences may be critical and very relevant [19]. Since a few cells with little damage would hardly influence the mean damage of a cancer cell population, it is beneficial to consider the full distribution of damage within the population rather than the mean (or any other aggregate, e.g. the median damage). It is equally important to consider how this distribution changes over time. The methodology presented here has therefore been specifically designed to bridge the gap between the experimental readout and the model structure in a fashion that takes into account the damage-distribution in a time-resolved manner.

Following a model-based strategy calls for a set of tools, specifically (a) a mathematical model able to predict DNA damage and its repair; (b) a methodology to obtain DNA damage readout experimentally from irradiated cells, i.e. to quantify DNA damage; and (c) a way to map and compare the model prediction (a) to experimental results (b). The contribution of this work is as follows. First, a method (c) to map experimentally obtained DNA damage readout (b, based on comet assay) to a DNA damage- and repair-model (a, the Multi-Hit-Repair model [14]) is presented, attributing particular care to the stochastic nature of the readout. This mapping also takes into account the dynamic nature of the repair process by considering measurements taken in a time-resolved manner. Second, the properties of the model (a) and the readout (b) necessary for a successful mapping are discussed to generalize these findings to other research

questions. Third, parameter search is performed on such data, showcasing the potential of this method.

## 2 Methods

In this section, the various methods used in this work are described. Sec. 2.1 outlines how the cells are treated during the experiment. Sec. 2.2 describes the comet assay, a method to quantify DNA damage. In Sec. 2.3, the Multi-Hit-Repair model is presented, which is the mathematical model used to predict DNA damage and repair. Sec. 2.4 describes how experimentally quantified DNA damage is mapped to the prediction of the model. These three sections correspond to the three key-aspects (b), (a) and (c) mentioned in the in introduction. Lastly, an approach for parameter search is presented in Sec. 2.5.

### 2.1 Experimental Setup

A canine osteosarcoma cell line (Abrams) is kept in culture at 37 °C. At the beginning of the experimental procedure, cells and medium are transferred to cell culture dishes. One dish is used for each time-point. The dishes containing the cells and medium are irradiated at 6 Gy with a clinical linear accelerator (Clinac iX, Varian, Palo Alto, CA, USA) operating at a dose rate of 6 Gy/min. Using the comet assay, DNA damage is quantified before, as well as 15, 30, 60, 120, 240 and 360 min. after irradiation.

### 2.2 Comet Assay

The comet assay (also referred to as single cell gel electrophoresis assay, Trevigen, Gaithersburg, MA, USA) is a method to assess the amount of damage in DNA [13]. Cells are dispersed and suspended in agarose gel and lysed, thus dissolving cellular membranes, proteins, RNA and other cell constituents. At the end of this step, only unwound DNA is left. Then, electrophoresis is performed; DNA fragments are dragged towards the positive electrode. The smaller a fragment, the easier it can move through the gel and the farthest it has moved after the completion of the electrophoresis step. At this stage, structures resembling comets can be observed by fluorescence microscopy. The fragments form a comet tail shape, facinng away from the bulk of DNA, which looks like a comet head. Sample comets are shown in Fig. 1. The standard Trevigen protocol was used for this procedure, specifically following recommendations for obtaining reliable and repeatable results [6].

Each cell embedded into the gel forms one comet. Thus, DNA damage is quantified on a per-cell basis from the resulting microscopy image by computing the relative pixel intensity of the tail compared to the total pixel intensity of the comet structure, i.e.

$$\text{Relative tail intensity} = \frac{\sum_{x,y\in\text{tail}} I(x,y)}{\sum_{x,y\in\text{head}} I(x,y) + \sum_{x,y\in\text{tail}} I(x,y)} \tag{1}$$

$I(x, y)$ denotes the pixel intensities at coordinates $x$ and $y$. The Comet IV software was used to quantify the relative tail intensity of approx. 100 randomly selected cells for each of the 7 time-points.

### 2.3 Multi-Hit-Repair (MHR) Model

The MHR model [14] is a dynamic population model where cells are assigned to populations $H_i$ depending on the number of radiation-induced hits they have accumulated. Cells with one or more hits have lost their ability to form clones (clonogenicity). This implies that a hit is defined as a lesion which prevents cells from undergoing mitosis. Regarding DNA, the MHR model does not impose what a hit consists of. In particular, one hit does not correspond to one DNA break, but it can be assumed that more hits generally correspond to more damage. As illustrated in Fig. 1, the populations are arranged in a chain structure. Initially, all cells are assigned to population $H_0$ which represents cells able to undergo mitosis – they are clonogenic. Damage is induced at a rate $\alpha R(t) \cdot H_0$ where $R(t)$ is the dose rate of irradiation. It is set to 0 Gy/min. prior to and after irradiation and has a value of 6 Gy/min. during irradiation. Irradiation starts at $t = 0$ min., and its duration is such that the target dose of 6 Gy is reached.

Population $H_1$ contains cells that have accumulated one hit, $H_2$ contains cells with two hits, etc. According to the definition of a hit, these cells cannot undergo mitosis. When a hit of a cell in population $H_i$ is repaired, the cell is transferred to population $H_{i-1}$. Damaged cells in the $H_i$ populations can also undergo cell death at a rate of $c_e H_i$, which occurs when a damaged cell fails to repair itself and dies instead. The repair rate is a function of $H_i$, the repair rate constant $c_r$ and the repair inhibition due to radiation-induced protein damage (see below). These various contributors to the repair rate are all summarized in the repair function $r(H_i)$. Thus, the differential equations for population $H_i$ is:

$$\frac{\mathrm{d}H_i}{\mathrm{d}t} = \alpha R(t) H_{i-1} - \alpha R(t) H_i - r(H_i) + r(H_{i+1}) - c_e H_i \tag{2}$$

Since radiation induces protein damage, such damage in DNA repair proteins must be cured before DNA repair can occur. This is modeled with a transient biological dose equivalent (TBDE) $\Gamma$. After irradiation, repair proteins are impaired, resulting in a high TBDE. As time progresses, these proteins are repaired, the TBDE drops and DNA repair starts to take place. This is modeled as follows:

$$\frac{\mathrm{d}\Gamma}{\mathrm{d}t} = R(t) - \gamma\Gamma \tag{3}$$

$$r(H_i) = c_r \exp\left(-\mu_\Gamma \Gamma\right) H_i \tag{4}$$

The derivation of these equation along with further discussion and validation of the model can be found in [14]. Initial conditions are $H_0(0) = 1$, $H_{i>0}(0) = 0$ and $\Gamma(0) = 0$, assuming that no damage is present before irradiation. In cases

where this assumption is violated, $H_i(0)$ can also bet set according to the pre-existing damage (see Sec. 3). The full set of equations is given in Fig. 1. A summary of the model parameters is presented in Tab. 1.

**Table 1.** Summary of model parameters with their respective search space boundaries. The last column indicates the result of parameter search. For completeness, the dose rate $R(t)$ is also given. It is not determined during parameter search, but rather fixed to reflect the experimental conditions. The fit error $\epsilon$ (as defined in Sec. 2.5) is 0.06.

| Parameter | Description | Min. | Max. | Fit |
|---|---|---|---|---|
| $\alpha$ | Radiosensitivity ($\mathrm{Gy}^{-1}$) | 0 | 2 | 0.09 |
| $c_r$ | Repair rate constant ($\mathrm{h}^{-1}$) | 0 | 10 | 0.22 |
| $c_e$ | Elimination rate constant ($\mathrm{h}^{-1}$) | 0 | 10 | 0.00 |
| $\mu_\Gamma$ | TBDE weighting factor ($\mathrm{Gy}^{-1}$) | 0 | 10 | 0.00 |
| $\gamma$ | TBDE rate constant ($\mathrm{h}^{-1}$) | 0 | 10 | 3.80 |
| $R$ | Dose rate ($\mathrm{h}^{-1}$) | $\begin{cases} 360 & 0\ \mathrm{h} \le t \le \frac{1}{60}\ \mathrm{h} \\ 0 & \text{otherwise} \end{cases}$ | | |

### 2.4 Relationship Between Comet Assay Readout and Model State

At any point in time $t$, the state variables $H_i$ quantify the fraction of the cell population that has accumulated $i$ hits ($0 \le i \le K$). This is a consequence of choosing the initial conditions such that 100 % of the cells are in $H_0$ initially ($H_0(0) = 1$). Conversely, the comet assay readout is a number $d_j$ for each of the $m$ cells that are quantified. Since $d_j$ is a relative tail intensity as defined in Eq. 1, $0 \le d_j \le 1$.

Because of the assumption that an increasing amount of DNA damage $d_j$ translates to a higher number of hits $i$, a strategy where the populations $H_i$ are mapped to histogram frequency bins of the distribution of $d_j$ in an ordered fashion appears to be the obvious choice. This mapping, however, implies that a specific range of DNA damage (e.g. 0 % – 5 %) is mapped to a population (e.g. $H_0$). Since the model imposes that only the $H_0$ population can undergo mitosis, the choice of range is not arbitrary. As explained below, calibration of a scaling factor $s$ is required to ensure a correct relationship.

More formally, the mapping is achieved as follows for every time-point $t$: First, the $m$ comet assay readouts $d_j$ are scaled with a scaling factor $s$, i.e. $\tilde{d}_j = s \cdot d_j$. This is done to establish the correct relationship between the DNA damage frequency bins and the model populations. Second, all $\tilde{d}_j$ are binned into $K + 1$ bins such that the $i$th bin $r_i$ contains the number of $\tilde{d}_j$ with a damage between $\frac{i}{K}$ and $\frac{i+1}{K}$. These histogram bins $r_i$ sum up to $m$ and are then normalized to the bins $\tilde{r}_i$ which sum up to 1. In a third step, the cell populations $H_i$ are normalized in the same way, such that

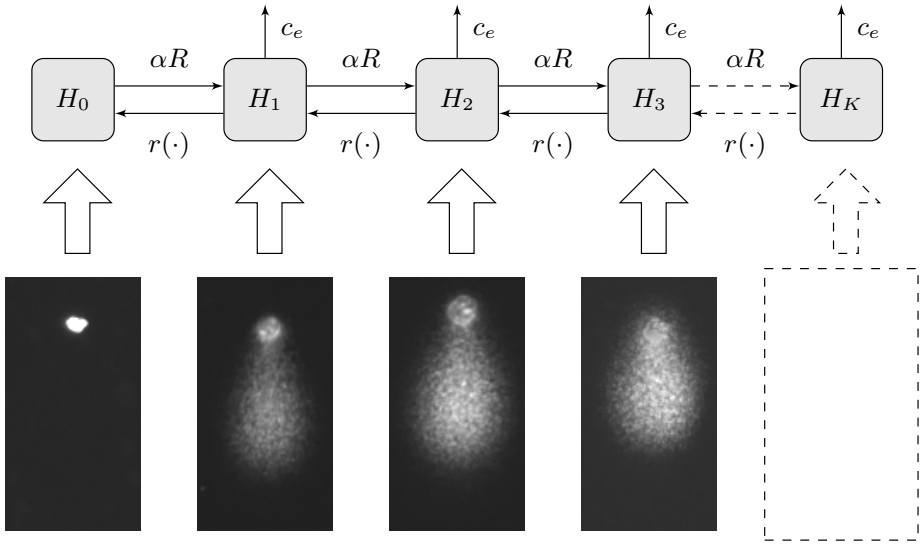


$$
\begin{aligned}
\frac{\mathrm{d}H_0}{\mathrm{d}t} &= -\alpha R H_0 + r(H_1) \\
\frac{\mathrm{d}H_1}{\mathrm{d}t} &= \alpha R H_0 - \alpha R H_1 - r(H_1) - c_e H_1 + r(H_2) \\
&\dots \\
\frac{\mathrm{d}H_{i-1}}{\mathrm{d}t} &= \alpha R H_{i-2} - \alpha R H_{i-1} - r(H_{i-1}) - c_e H_{i-1} + r(H_i) \\
\frac{\mathrm{d}H_i}{\mathrm{d}t} &= \alpha R H_{i-1} - \alpha R H_i - r(H_i) - c_e H_i + r(H_{i+1}) \\
\frac{\mathrm{d}H_{i+1}}{\mathrm{d}t} &= \alpha R H_i - \alpha R H_{i+1} - r(H_{i+1}) - c_e H_{i+1} + r(H_{i+2}) \\
&\dots \\
\frac{\mathrm{d}H_K}{\mathrm{d}t} &= \alpha R H_{K-1} - r(H_K) - c_e H_K \\
\frac{\mathrm{d}\Gamma}{\mathrm{d}t} &= R - \gamma \Gamma \\
r(H_i) &= c_r \exp\left(-\mu_\Gamma \Gamma\right) H_i
\end{aligned}
$$

**Fig. 1.** Top: High-level illustration of the MHR model. The boxes depict the chain structure with the populations $H_i$; the arrows denote how cells accumulate hits (to the right), undergo cell death (to the top) or undergo repair (to the left). Below the chain, comet assay pictures conceptually illustrate how comets with increasingly high relative tail intensities are mapped to populations with increasingly high numbers of hits. Bottom: Below the illustration, the full set of system equations is given. (See [14] for details.)

$$\sum_{i=0}^{K} \tilde{r}_k = \sum_{i=0}^{K} \tilde{H}_i = 1 \ . \tag{5}$$

This normalization is necessary to overcome the fact that dead cells are eliminated in the model, thus reducing $H_i$, while the experimentally obtained damage readouts are always performed on approx. 100 cells.

Finally, to compare comet assay readout and model state, the normalized cell populations $\tilde{H}_i$ are mapped to the damage readout bins $\tilde{r}_i$ in a pairwise fashion. This technique allows for a comparison in distribution rather than just mean values. In general, the length of the chain $K$ is not critical provided that it is sufficiently long [14] – in an excessively long chain, populations with a high number of hits simply remain empty. In the simulation presented here, a value of $K = 24$ was chosen. The scaling factor $s$ was fixed to 1 for now, mapping DNA damage between 0 % and 4 % to $H_0$, damage between 4 % and 8 % to $H_1$ etc. The choice of $s$ is non trivial and remains a challenge, thus strategies to determine $s$ are discussed in Sec. 4.

### 2.5 Parameter Search

Differential evolution [16] was used to perform parameter search by minimizing the sum of squares

$$\epsilon = \sum_{t>0} \sum_{i=0}^{K} \left( \tilde{r}_i^{(t)} - \tilde{H}_i(t) \right)^2 \tag{6}$$

where $\tilde{r}_i^{(t)}$ denotes the $i$th normalized histogram bin at time point $t$. The time-points $t \in (15, 30, 60, 120, 240, 360)$ min. are considered for the minimization, but not the time-point $t = 0$ min. (i.e. before irradiation) since no parameter has any effect on the model-prediction at $t = 0$ min.

The model was implemented using Python 3.6.6 and employing the `odeint()` function from version 1.1.0 of the `scipy` python package. Differential evolution was performed with the `differential_evolution()` of the same package.

## 3 Results

Fig. 2 shows experimental results from comet assays (top) along with the model prediction (bottom) after parameter search. The resulting model parameters are listed in Tab. 1. Parameter search took approx. 10 min. on a 2.0 GHz Intel Xeon core and reliably converged to always the same endpoints with an error of $\epsilon = 0.06$.

As expected, the damage increases after irradiation both in the experimental readout (top half of Fig. 2) as well as in the model prediction (bottom half of Fig.

2). The violin-like structures in the plot show the statistical density of the data; when the violin is wide, a high number of values are present in the corresponding range of relative tail intensities. The violins of the model prediction are jagged due to the discrete nature of the populations. For the experimental data, the violins are generated from the readout without binning (i.e. from $\tilde{d}_j$), thus the violin outlines are smoother. The comet assay readout before irradiation suggests that the assumption of no damage prior to irradiation is false – some damage is present even before irradiation. The initial conditions for $H_i$ were set according to the distribution of this readout.

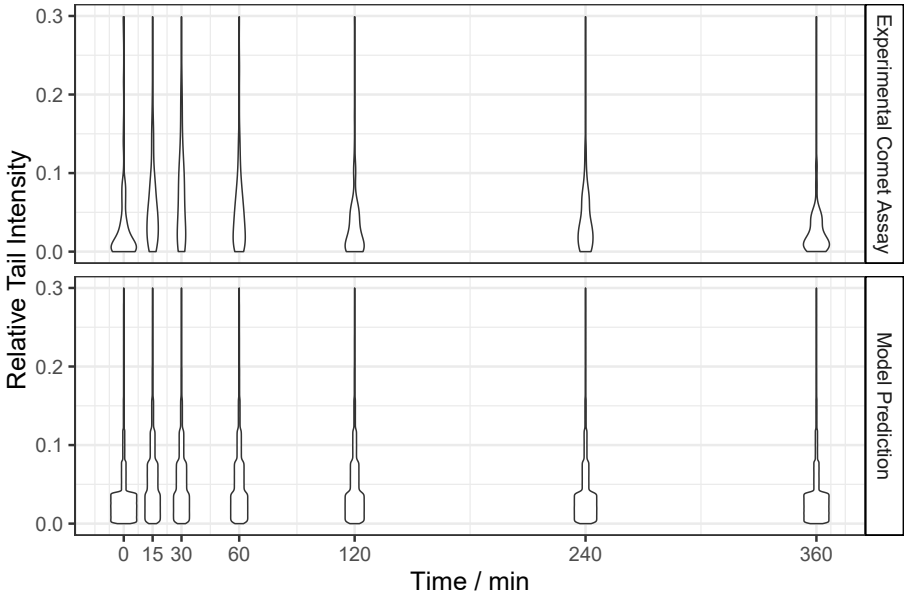


**Fig. 2.** Violin plots of comet assay readouts after irradiation with 6 Gy (top) and corresponding model prediction (bottom) of Abrams osteosarcoma cells. The readout at $t = 0$ min. is acquired immediately before irradiation. The vertical axis is limited to the range between 0 % and 30 % of relative tail intensity.

## 4 Discussion and Conclusion

The results showcase that the MHR model is able to produce output that is in line with DNA damage readouts obtained with comet assays after irradiation. Thus, the strategy proposed in this work appears to be a viable candidate to map experimental DNA damage readout to the MHR model state and back, and

more generally, to grasp the distribution of aspects of populations that change over time.

So far, most parameter searching has been performed based on clonogenic cell survival curves, i.e. dose-response curves that assess for each dose the proportion of cells which survived irradiation and were able to form clones [14, 18]. This proportion corresponds to $\lim_{t\to\infty} H_0(t)$ in the MHR model, i.e. the fraction of initial cells that have fully recovered from the irradiation and have regained their ability to undergo mitosis. Thus, $H_0(t)$ is evaluated many hours after the essential dynamics have ceased. Doing so introduces an undesired ambiguity: as long as the duration of irradiation is short compared to the repair process, parameters can be scaled in the time-domain without affecting the end result. For example, reducing $c_r$ by a factor of e.g. 10 would eventually yield the same surviving proportion provided that other parameters are scaled accordingly. The process would take longer, but this has no effect on the proportion of surviving cells since only the end-point is evaluated. In fact, such ambiguities in the prediction of cell survival curves have been found [18] and prompted for the time-resolved approach introduced here.

While such a time-resolved approach does remove the aforementioned ambiguity, the scaling factor $s$ is required to determine the scaling in the damage/hit-domain. $s = 1$ was used for the parameters reported in Tab. 1, linking clonogenic cells to relative tail intensities of 0 % – 4 %. As discussed above, other ranges are equally reasonable; the yet unknown scaling factor $s$ is required to render the results from parameter search comparable to parameter values estimated from cell survival curves. It is critical to note that finding a suitable scaling factor would still produce the results shown in Fig. 2, but the parameter values would change, allowing for a comparison with values found and reported in the past. Unfortunately, it is not possible to calibrate $s$ from comet assay readouts because these readouts do not carry any information on the clonogenicity of the cells. This information, however, is required because $H_0$ must contain clonogenic cells by definition. Hence, a parameter search with combined data from comet assay and clonogenic assay should be used instead.

Interestingly, both the elimination rate constant $c_e$ as well as the TBDE weighting factor $\mu_\Gamma$ converged to 0, which was the lower bound of the search space. A possible explanation for a low $c_e$ is that the normalization introduced in Eq. 5 in order to compensate for the fact that a fixed number of cells are examined in the comet assay, thus disregarding a reduction of the overall number of remaining living cells, conceals cells that have been eliminated. Moreover, cell death is a process that takes time, and the 6 hours of simulation may simply not extend to the point in time at which cell death occurs. These findings again prompt for a combined analysis with both comet assay and clonogenic assay because the latter inherently captures cell survival.

The estimate of $\mu_\Gamma$=0 $\mathrm{Gy}^{-1}$ is challenging to interpret, since a slow-down or even stall of repair directly after irradiation is a plausible and well established phenomenon [15], which is thought to be a combination of time required to recruit DNA repair proteins before DNA repair can start and time required to

repair such proteins that may have been damaged by radiation. Setting $\mu_\Gamma = 0\ \mathrm{Gy}^{-1}$ eliminates this phenomenon from the model, suggesting that efforts should be put into investigating how relevant and robust this parameter is. A potential method to achieve this could be approximate bayesian computation (ABC) [1], where parameters search does not yield point-estimates, but rather results in distributions of parameters in the search space.

For a successful application of the method presented here, the readout should reflect the quantity that is modeled. In the context of DNA damage and repair, this entails that the readout correlates well with the damage introduced by radiation. While the correlation between primary damage and radiation dose is well established [2, 12], the practice of quantitatively inferring DNA damage from a microscopy image of cells subject to the electrophoresis process may appear questionable at first. However, an excellent linear relationship between the applied radiation dose and the relative tail intensity was found, with coefficients of determination exceeding $R^2 = 0.95$ [8, 17]. One may generally question whether comet assay is the best technique to investigate DNA damage and response in quantitative terms. A popular alternative would be the use of $\gamma$H2AX, a biomarker for double strand breaks [9]. However, the $\gamma$H2AX response is delayed by up to 30 min. and remains detectable after the double strand break has been repaired, and the relationship between applied dose and response is worse than with comet assay [7, 11]. The first issue in particular renders $\gamma$H2AX an inferior alternative to comet assay since the readout should reflect the current state of the system rather than some time-delayed state.

Similarly, one may question whether the MHR model is a suitable choice for the task at hand. Most models commonly used in radiobiology do not model DNA damage and repair kinetics. Instead, they model the observed outcome directly. For example, the linear-quadratic model [4, 10] and the linear-quadratic-liner model [5] describe the relationship that is observed between dose and surviving fraction of cells. They do not relate to radiobiological principles but merely reflect the observed outcome. Thus, they cannot be used in this context. The MHR model, on the other hand, is a suitable choice because it is designed with radiobiological concepts from the ground up. In consequence, the topology of the model can be mapped to the distribution of damage-readouts, as demonstrated in this work.

In conclusion, the method presented here appears to be suitable for bridging the gap between the time-resolved comet assay readout and the MHR model because it tackles the key difficulty of the problems, which is to treat the readout as a distribution and to establish a relationship between this distribution and the model populations. In a next step, the scaling factor $s$ should be calibrated using the proposed multi-assay parameter search, consisting of both comet- as well as clonogenic assay, followed by validation of the model and the mapping.

## Funding

This work was supported by the Swiss National Foundation (grant number 320030_163435) – Stephan Scheidegger; Carla Rohrer Bley.

## References

1. Albert, C., Künsch, H.R., Scheidegger, A.: A simulated annealing approach to approximate bayes computations. Statistics and computing **25**(6), 1217–1232 (2015)
2. Barnard, S., Bouffler, S., Rothkamm, K.: The shape of the radiation dose response for dna double-strand break induction and repair. Genome integrity **4**(1), 1 (2013)
3. Besserer, J., Schneider, U.: A track-event theory of cell survival. Zeitschrift fuer Medizinische Physik **25**(2), 168–175 (2015)
4. Dale, R.G.: The application of the linear-quadratic dose-effect equation to fractionated and protracted radiotherapy. The British journal of radiology **58**(690), 515–528 (1985)
5. Guerrero, M., Li, X.A.: Extending the linear–quadratic model for large fraction doses pertinent to stereotactic radiotherapy. Physics in Medicine & Biology **49**(20), 4825 (2004)
6. Hartmann, A., Agurell, E., Beevers, C., Brendler-Schwaab, S., Burlinson, B., Clay, P., Collins, A., Smith, A., Speit, G., Thybaud, V., et al.: Recommendations for conducting the in vivo alkaline comet assay. Mutagenesis **18**(1), 45–51 (2003)
7. Kinner, A., Wu, W., Staudt, C., Iliakis, G.: $\gamma$-h2ax in recognition and signaling of dna double-strand breaks in the context of chromatin. Nucleic acids research **36**(17), 5678–5694 (2008)
8. Kumaravel, T., Jha, A.N.: Reliable comet assay measurements for detecting dna damage induced by ionising radiation and chemicals. Mutation Research/Genetic Toxicology and Environmental Mutagenesis **605**(1), 7–16 (2006)
9. Kuo, L.J., Yang, L.X.: $\gamma$-h2ax-a novel biomarker for dna double-strand breaks. In vivo **22**(3), 305–309 (2008)
10. Lea, D.E.: Actions of radiations on living cells. Cambridge University Press.; Cambridge (1946)
11. Mariotti, L.G., Pirovano, G., Savage, K.I., Ghita, M., Ottolenghi, A., Prise, K.M., Schettino, G.: Use of the $\gamma$-h2ax assay to investigate dna repair dynamics following multiple radiation exposures. PloS one **8**(11), e79541 (2013)
12. Mori, R., Matsuya, Y., Yoshii, Y., Date, H.: Estimation of the radiation-induced dna double-strand breaks number by considering cell cycle and absorbed dose per cell nucleus. Journal of radiation research **59**(3), 253–260 (2018)
13. Olive, P.L., Banáth, J.P.: The comet assay: a method to measure dna damage in individual cells. Nature Protocols **1**, 23–29 (2006)
14. Scheidegger, S., Fuchs, H.U., Zaugg, K., Bodis, S., Füchslin, R.M.: Using state variables to model the response of tumour cells to radiation and heat: a novel multi-hit-repair approach. Computational and mathematical methods in medicine **2013** (2013)
15. Schulz, N., Chaachouay, H., Nytko, K.J., Weyland, M.S., Roos, M., Füchslin, R.M., Guscetti, F., Scheidegger, S., Rohrer Bley, C.: Dynamic in vivo profiling of dna damage and repair after radiotherapy using canine patients as a model. International journal of molecular sciences **18**(6), 1176 (2017)

16. Storn, R., Price, K.: Differential evolution–a simple and efficient heuristic for global optimization over continuous spaces. Journal of global optimization **11**(4), 341–359 (1997)
17. Wang, Y., Xu, C., Du, L.Q., Cao, J., Liu, J.X., Su, X., Zhao, H., Fan, F.Y., Wang, B., Katsube, T., et al.: Evaluation of the comet assay for assessing the dose-response relationship of dna damage induced by ionizing radiation. International journal of molecular sciences **14**(11), 22449–22461 (2013)
18. Weyland, M., Thumser-Henner, P., Nytko, K., Rohrer Bley, C., Füchslin, R., Scheidegger, S.: Proceedings: Extracting information about cellular repair processes after hyperthermia – radiotherapy by model-based data analysis – ambiguities in survival prediction as a challenge? Strahlenther Onkol **194**(5), 503–504 (2018)
19. Zaider, M., Hanin, L.: Tumor control probability in radiation treatment. Medical physics **38**(2), 574–583 (2011)